Send Orders for Reprints to reprints@benthamscience.ae

Letters in Organic Chemistry, **2019**, *16*, 000-000

RESEARCH ARTICLE

Preparation and Physicochemical Characterization of Inclusion Complexes Derived from Phytosterols and β-cyclodextrin

Ana Lía Rossi[1], Adriana Mabel Rosso[2], Eduardo Miguel Rustoy[1,3*] and Gabriel Cases[3]

[1]*Laboratorio de Química Orgánica. Departamento de Ciencias Básicas. Universidad Nacional de Luján. Ruta 5 y Avenida Constitución, C.C. 221, B6700AVW, Luján, Buenos Aires. Argentina;* [2]*Laboratorio de Química Biológica. Departamento de Ciencias Básicas. Universidad Nacional de Luján. Ruta 5 y Avenida Constitución, C.C. 221, B6700AVW, Luján, Buenos Aires. Argentina;* [3]*Departamento de Química Orgánica y UMYMFOR, Facultad de Ciencias Exactas y Naturales, Universidad de Buenos Aires-CONICET, Pabellón 2, Piso 3, Ciudad Universitaria, C1428EGA Buenos Aires, Argentina*

ARTICLE HISTORY

Received: April 12, 2018
Revised: June 08, 2018
Accepted: June 20, 2018

DOI:
10.2174/1570178615666180629102223

Abstract: Phytosterols (PS), that is vegetable sterols, are compounds widely recognized for lowering the absorption of cholesterol and decreasing cancer risk, with βsitosterol, stigmasterol and campesterol being the most abundant. As PS is poorly soluble in aqueous solutions, many approaches have been proposed to increase their solubility and bioavailability. β-cyclodextrin (β-CD) could be used to increase PS aqueous solubility because of its capacity to entrap a variety of hydrophobic guest molecules in its cavity. In this work, the formation of β-CD/PS inclusion complexes was confirmed by differential scanning calorimetry (DSC), electrospray ionization-high resolution mass spectrometry (ESI-HRMS) and Fourier transform infrared spectroscopy (FT-IR), while structural characteristics were determined by one- and two-dimensional nuclear magnetic resonance (NMR) techniques. Results confirmed 1:1 binding stoichiometry, which suggests the total inclusion of rings and chains of the different PS. The hypothesis of folding of the lateral chains into the cavity may be supported by the multiple correlations observed in the nuclear Overhauser effect spectroscopy (NOESY) and rotating-frame nuclear Overhauser effect spectroscopy (ROESY) spectra.

Keywords: Phytosterols, β-cyclodextrin, inclusion complex, NMR spectroscopy, ESI-HRMS.

1. INTRODUCTION

Phytosterols (PS), *i.e.* plant sterols and stanols, are structurally similar to cholesterol but exclusively synthesized by plants, and include β-sitosterol (βS), campesterol (C) and stigmasterol (S) in the largest proportion in most sources. The interest in studying PS was initially sparked by their effectiveness in reducing the absorption of dietary cholesterol and thus offering protection from cardiovascular diseases [1-4]. PS is adsorbed proportionally to cholesterol but to a much lesser extent (5). The most prevalent PS, βS has been well documented in medical research and has been reported to possess cholesterol-lowering properties. Some studies have also demonstrated that daily consumption of βS is associated with decreased cancer risk [6,7].

Controlled dietary studies in animals suggest that PS may offer protection against breast, colon and prostate cancer, among others. An interesting hypothesis which may account for this protective action is that PS induces apoptosis or programmed cell death in proliferative tumor cells [7].

Although PS is widely found in the normal diet, the amounts usually acquired are barely adequate to render significant health benefits. The natural background intake of free PS and phytostanols from plant products, including seeds, nuts and vegetable oils, has been estimated to be within a range of 150-400 mg/day. As the cholesterol-lowering effects of free PS and phytostanols reach a plateau at approximately 2g/person per day, these compounds become interesting food supplements and ingredients in food formulation. The use of PS, phytostanols and their esters is regulated in numerous countries including the EU, USA, Australia and New Zealand, either as food additives/ ingredients or as supplements [8]. However, the incorporation of these compounds in food and their administration as therapeutic tools is still limited because they are more easily soluble in fats and oils than in aqueous solutions. Therefore, many approaches have been proposed to increase the solubility or bioavailability of PS, such as PS ester synthesis, emul-

*Address correspondence to this author at the UMYMFOR-Departamento de Química Orgánica, FCEyN, CONICET-UBA, P.O. Box: C1428EGA, Ciudad Autónoma de Buenos Aires, Argentina; Tel/Fax: +54-11-4576-3385; E-mail: erustoy@yahoo.com.ar

1570-1786/19 $58.00+.00

sion formulation and nano-size dispersion [9-12]. These approaches enable the convenient incorporation of PS as food additives without adverse organoleptic effects.

Along the same lines, molecular encapsulation could also be used to increase the aqueous solubility of poorly soluble compounds and to enhance their bioavailability and stability [13, 14]. In particular, cyclodextrins (CD) can be employed as encapsulation agents because of their capacity to entrap a variety of hydrophobic guest molecules of suitable size in their cavity, thus leading to the formation of inclusion complexes [15, 16].

CD is cyclic oligosaccharides containing six (α-CD), seven (β-CD) or eight (γ-CD) α -1, 4 glucopyranose units linked. Their molecules are shaped like truncated cones with a central cavity where the hydroxyl groups are oriented to the exterior of the cavity, with the secondary hydroxyl groups located in the larger opening and the primary ones in the smaller opening. The three-dimensional structure of CD molecules gives the outer surface a hydrophilic character and water solubility. In contrast, the inner cavity is lined by hydrogen atoms and glycosidic oxygen bridges presenting a relatively hydrophobic character. This cavity can receive other lipophilic guest molecules, provided they have the correct size and shape.

As α-, β- and γ-CD have now generally recognized as Safe (GRAS) status and have been recently approved as additives in the EU, CD can be easily used in the food industry [16]. Also, CD is used as drug carriers in the pharmaceutical industry to enhance the solubility and stability of bioactive molecules and has been approved by the Food and Drug Administration (FDA) as being friendly to humans [15]. After oral administration, the natural CD and their derivatives are susceptible to bacterial digestion in the gastrointestinal tract. Whereas α- and β-CD are predominantly digested by bacteria in the colon, γ-CD is rapidly digested by salivary and pancreatic α amylase. On the other hand, after parenteral administration, CD is mostly excreted unchanged in the urine *via* glomerular filtration [17]. For these and other reasons, CD is now widely employed in pharmaceutical, cosmetics, food and chemistry industrial sectors [17, 18].

The suitable characterization of CD esterols and steroids inclusion complexes and the assessment of their formation in the solid state require joint use of different analytical techniques, whose combined analysis may enable an appropriate and in-depth understanding of host-guest interactions [19]. In this context, the objectives set out in this work were first to obtain a mixture of inclusion complexes formed by β-CD and a mixture of PS-rich in βS with minor amounts of S and C. Secondly, we aimed to establish stoichiometric host-guest relationships in each of the inclusion complexes formed, elucidating the mode in which PS is included in the β-CD and whether the process involves any degree of selectivity according to PS structural differences. This analysis may pose operational obstacles, as obtaining a mixture of inclusion complexes with a concentration and molar ratio of PS similar to those presented by the original mixture, prepared according to the range of concentrations recognized as their nutritional contribution, requires each of the complexes to be prepared separately and then mixed in the desired molar ratio. Spectroscopic tools used to characterize inclusion complexes and demonstrate host-guest interaction included differential scanning calorimetry (DSC), electrospray ionization-high resolution mass spectrometry (ESI-HRMS), Fourier-transform infrared spectroscopy (FT-IR) and one- and two-dimensional nuclear magnetic resonance (NMR) techniques.

2. RESULTS AND DISCUSSION

2.1. GC Analysis

In previous work, we studied (see Experimental) the effect of process parameters on EE as the concentration ratio of PS (mixture of PS-rich in β-S with minor amounts of S and C) and β-CD, temperature, time and speed of agitation. EE was determined by GC analysis of PS (mixture) concentration and by the phenolphthalein method quantifying the free β-CD in the solution. A high 75% encapsulation efficiency (EE) was reached for PS in β-CD.

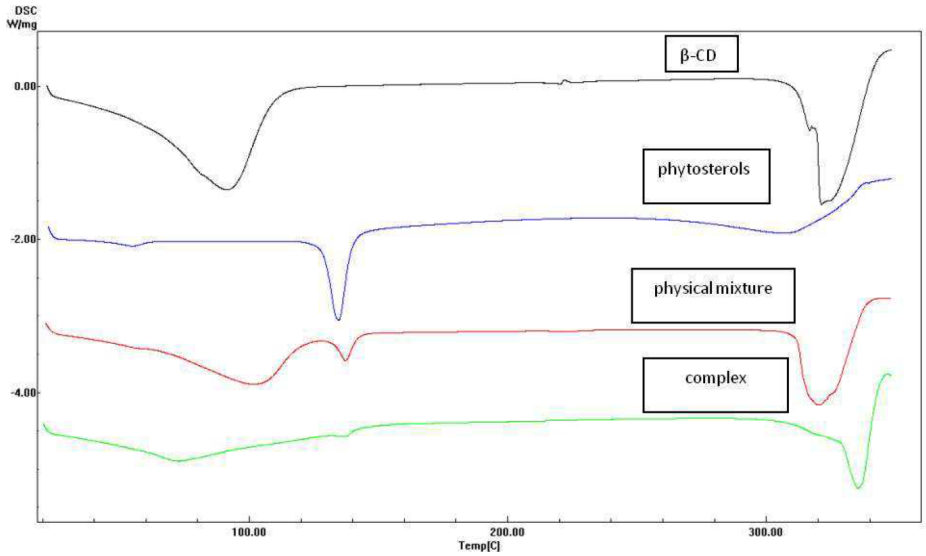

Fig. (1). DSC thermograms of β-CD, PS, β-CD-PS PM and β-CD-PS inclusion complexes.

2.2. DSC Analysis

DSC thermograms of β-CD, PS, β-CD-PS PM (physical mixtures) and β-CD-PS inclusion complex are shown in Fig. (**1**).

DSC can be used to measure the interaction between two components, as thermograms have been shown to change when guest molecules are included in the CD cavity. The points of melting, boiling and sublimation usually shift to a different temperature or disappear within the temperature range at which the CD is decomposed [20].

In the current analysis of β-CD, two endothermic peaks were observed in the thermogram centering at 91.36ºC and 321.67ºC, the first of which is assigned to the loss of crystal water from β-CD [21]. Likewise, analysis of the pure PS, complex and PM- *i.e*. both components not subjected to the process conditions for complex formation- revealed thermograms showing complex DSC curves different from those of the unreacted reagent mixture. The endothermic peak for PS at 134.72ºC corresponds to the melting point. Complex formation was proven by the absence of a sharp peak in the temperature range investigated, which was however present in the PM.

2.3. ESI-HRMS analysis

Figure (**2**) shows the area of interest of the ESI-HRMS (positive mode) β-CD/PS inclusion complex spectrum.

ESI-HRMS is a relatively soft ionization technique used for the analysis of biomolecules, which has become effective in determining molecular noncovalent interactions [22, 23]. This technique has therefore provided an opportunity to study the formation of inclusion complexes of CD with different organic molecules and several drugs [24, 25].

In the present study, the comparison of experimental and theoretical data confirms the presence of three inclusion complexes which have the same host-guest stoichiometric ratio, *i.e*. 1:1. These data support the conclusion that, although βS is a major component in the mixture of PS used, experimental conditions also allowed to find the inclusion complexes of PS to a lesser extent (S and C). This evidence receives further support from information obtained in the comparative NMR analysis of samples of free β-CD, the mixture of PS used as starting material and the corresponding inclusion complexes.

2.4. FT-IR Spectroscopy Analysis

Figure (**3**) shows the FT-IR spectra for the β-CD, PS, β-CD-PS PM and inclusion complexes.

FT-IR spectroscopy is used to analyze CD complex formation, as the bands for the guest and host molecules change intensity and position on complex formation [26-29].

An absorption band was also observed belonging to the valence vibrations of the C–H bonds in the CH and CH2 groups, with a maximum at 2926 cm^{-1}. The absorption bands from the deformation vibrations of the C–H bonds in the primary and secondary alcohol groups of β-CD and PS were observed in the region 1420–1300 cm^{-1}. The bands from the valence vibrations of the C–O bonds in the ether and hydroxyl groups of the CD were observed in the region 1210–1020 cm^{-1}. The absorption bands belonging to the deformation vibrations of the C–H bonds and the pulsation vibrations of the glucopyranose cycle were observed in the region 950-800 cm^{-1}. Broad signals were observed with maximums at 1647, 1666, 1645 and 1640 cm^{-1} for the four samples (Figs. **3A**, **B**, **C** and **D**), which reflect the δ-HOH bending of water molecules attached to CD, the PM and the complex [29b].

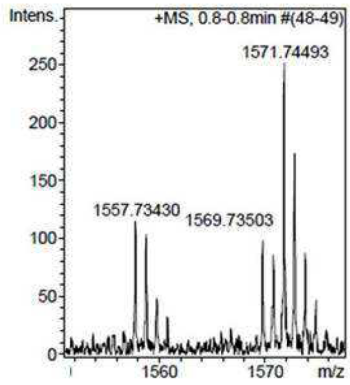

[Complex+Na]$^+$	Theorical m/z ratio [Da]	Experimental m/z ratio [Da] (error [ppm])	Molecular formula
[β-CD/C+Na]$^+$	1557.72950	1557.73430 [-3.08]	$C_{70}H_{118}NaO_{36}$
[β-CD/S+Na]$^+$	1569.72950	1569.73503 [-3.52]	$C_{71}H_{118}NaO_{36}$
[β-CD/βS+Na]$^+$	1571.74515	1571.74493 [0.14]	$C_{70}H_{120}NaO_{36}$

Fig. (2). Zone of the ESI-HRMS in a positive mode which rendered m/z (Z = 1) ratios [Da] of the β-CD-PS inclusion complexes spectra plus sodium $[M + Na]^+$.

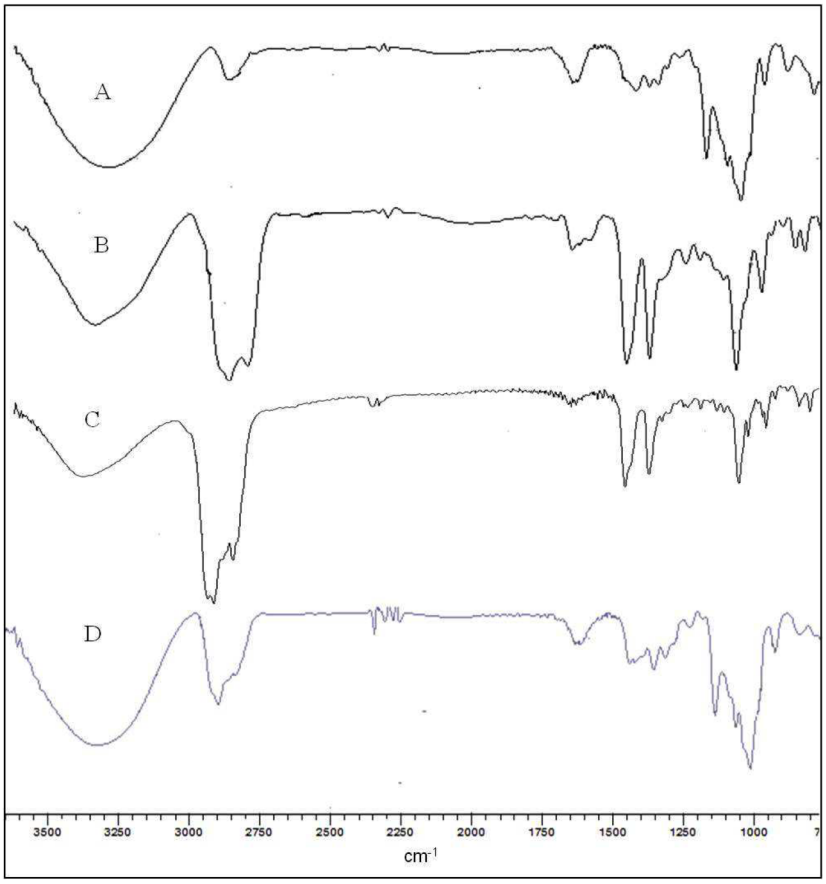

Fig. (3). FT-IR spectra of **A**: β-CD, **B**: PS, **C**: β-CD-PS PM, and **D**: β-CD/PS inclusion complexes.

Table 1. FT-IR signals of β-CD, PS (guest/s) and the inclusion complexes.

Functional Group	Wave Number (cm^{-1})			Changes $\Delta\nu$ (cm^{-1})
	β-CD	Guest/s	Inclusion Complexes	
$\nu_{(O-H)}$	3369		3369	0
$\nu_{(O-H)}$		3408	3369	-39
$\nu_{(=C-H)}$ (shoulder)		3042	Not observed	---
$\nu_{(C=C)}$		1652	1637	-15
$\nu_{(C-H)}$ (deformation)		1464	1458	-6
$\nu_{(C-H)}$ (deformation)	1411		1421	10
$\nu_{(C-H)}$ (deformation)		1373	1379	6
$\nu_{(C-O)}$	1157		1155	-2
$\nu_{(C-H)}$ (deformation, glucopyranose cycle)	947		941	-6

The FT-IR spectrum of PS mixture (Fig. **3B**) shows the following characteristic bands: 3408 (O-H); shoulder at 3032 (=CH); 2957, 2926, 2866 and 2853 (C-H bonds corresponding to CH and CH2 groups); 1652 (C=C); 1464-1300 (C-H, deformation vibrations) and 936 (OH) cm^{-1}.

The analysis of the spectrum of inclusion complexes (Fig. **3D**) presented difficulties due to overlapping host and guest signals. However, this may constitute evidence of their formation on the basis of displacement of diagnostic signals (Table **1**).

Table **1** shows increases and decreases in position bands, $\Delta\nu$ [cm^{-1}]. The increase was due to the insertion of a cyclic part into the electron-rich cavity of β-CD, which increases the density of the electron cloud and leads to an increase in frequency. The decrease in frequency between the inclusion complex and its constituent molecule was due to changes in

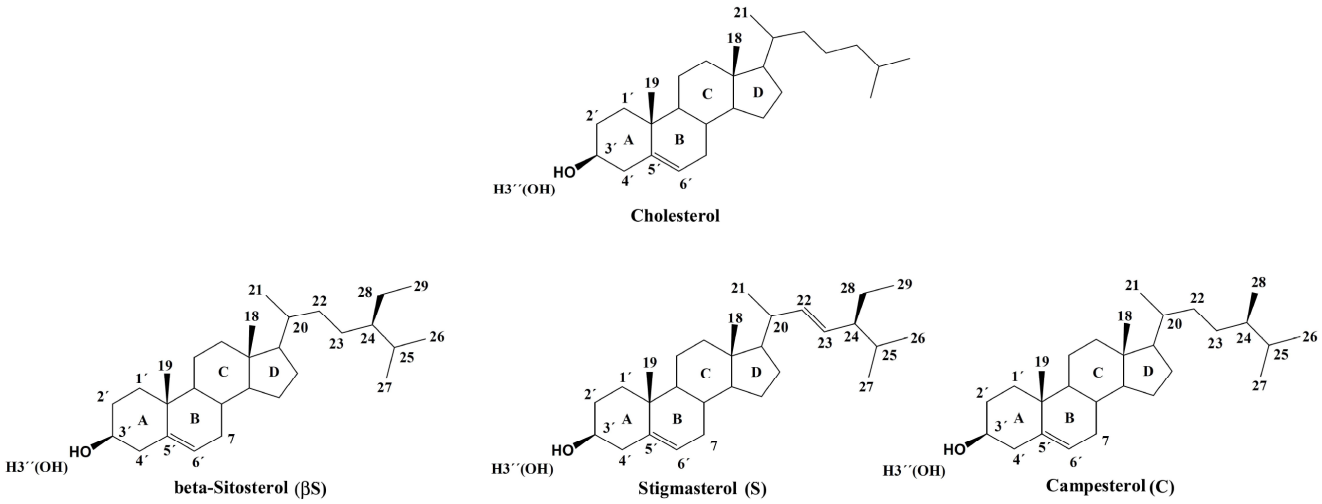

Fig. (4). Structures of cholesterol, β-sitosterol (βS), stigmasterol (S) and campesterol (C).

the microenvironment which lead to the formation of hydrogen bonding and the presence of van der Waals forces during their interaction to form the inclusion complex. On the other hand, the FT-IR spectrum of PM imitated the characteristic peaks of β-CD and βS/S/C, which can be regarded as a simple superimposition of those host and guest molecules. Thus, the FT-IR spectra conclusively proved the formation of inclusion complexes.

2.5. NMR Analysis

Host-guest interactions were also studied through the comparison of one- and two-dimensional NMR spectra of β-CD, PS and inclusion complexes recorded at 500.12 and 125 MHz for ^{1}H and ^{13}C, respectively, shown in Fig. (**4**). All spectra were acquired on samples prepared with the same solvent mixture (DMSO d_6/$CDCl_3$ 85:15 % v/v) in order to obtain consistent and comparable results, as different solvents or solvent mixtures may have rendered non comparable results due to the so-called specific and non-specific effects of the solvent on the molecules of a sample [31a-c]. In addition, spectroscopic ^{1}H-NMR data reported for cholesterol were recorded in DMSO d_6, to primarily establish the changes observed in the proton H(1′-4′), H3′(OH), H6′, H18, H19 and H21 (Fig. **4**) [32d]. To assign the ^{1}H and ^{13}C nuclei 1-7 and 18′-29′ for the case of βS and S, and the nuclei 1′-7′ and 18′-28′ of the same isotopes for C (Fig. 4), we used bibliographic information showing spectra of free PS [31e-f]. As the latter was acquired in $CDCl_3$ as the only solvent, the information obtained from them was used with guidance.

The data obtained from the one-dimensional ^{13}C and two-dimensional NMR spectra of β-CD and inclusion complexes allowed us to establish a single signal for each of the C nuclei in the inclusion complex, which may indicate that the interactions of the different guests with the same host were similar from a magnetic point of view. This assertion is based on bibliographical information reporting the high sensitivity of ^{13}C nuclei to minimum conformational changes which could be generated in free CD by the formation of inclusion complexes. As a next step, and on the basis of the bibliographical evidence mentioned above, the signals corresponding to protons H1-6 and H2′, 3′ and 6′(OH) (Fig. **5**) of the free host were assigned before and after complexation [31].

Scientific research has long focused on CD complexes by observing the chemical shifts of protons H3 and H5 inside the cavity of α-CD in the presence of residues of different molecules, for example, due to the anisotropic effect of an aromatic ring. A host-guest interaction leads to a change in the δ of hydrogens due to complexation [32,34a], which provides first evidence of the guest inclusion in the CD cavity [33].

In addition, the chemical shift variance of proton NMR proves that host and guest molecules interact with each other and form a complex. In this regard, it has been concluded that partial inclusion of the guest inside the cavity occurs when $\Delta\delta$ H3 > $\Delta\delta$ H5, while total inclusion takes place when $\Delta\delta$ H3 ≤ $\Delta\delta$ H5 [32, 34a]. As an example, the host-guest interactions of the inclusion complex [34a] Genistein/β-CD can be analyzed through the differences between proton chemical shifts of both species [35].

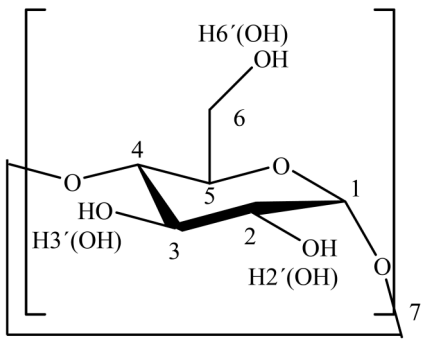

Fig. (5).

The present work also studied the qualitative effects of complex formation and the degree of guest inclusion in the

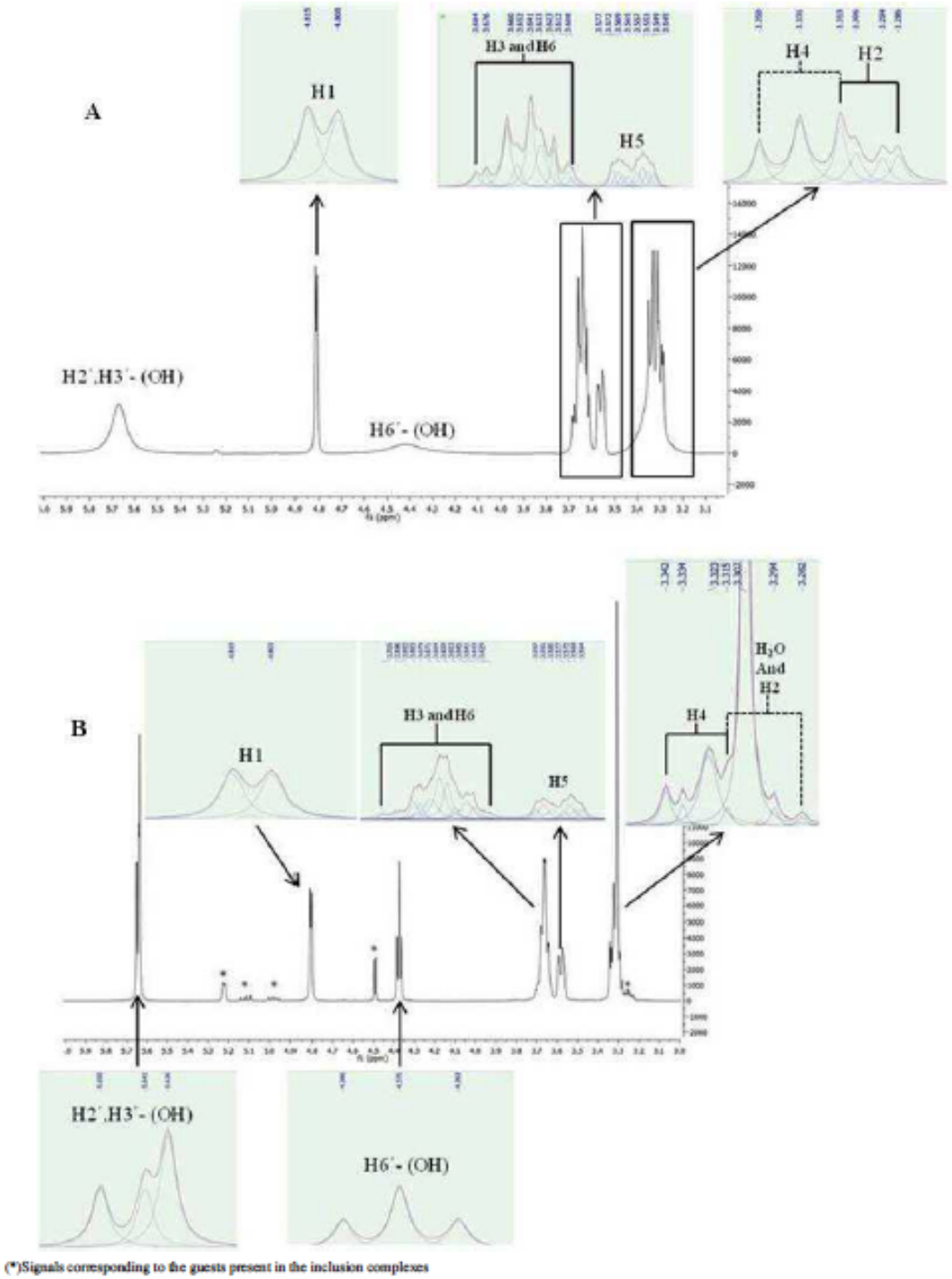

Fig. (6). 500 MHz ^{1}H-NMR spectra of free β-CD (A) and PS inclusion complexes (B) in DMSO d_6 (15 % $CDCl_3$) solvent mixture.

host cavity, in this case, β-CD. The ^{1}H-NMR spectra between 3.000 and 6.000 ppm of β-CD and its association with PS in the inclusion complex in DMSO d_6/$CDCl_3$ (85:15 % v/v) are shown in Fig. (**6**).

As the fields were around 500 MHz, only the anomeric protons (H1) exhibited enough separation from the others for an approximate first-order analysis of the ^{1}H-NMR spin system. Coupling constants for the other glucose protons can be accurately obtained by automated analysis of proton NMR spectra through global spectral deconvolution (GSD) as reported in the literature [34b, 36, 37].

^{1}H-NMR chemical shifts of the inclusion complex and the variance across those of β-CD are listed in Table **2**.

Considering the values of Δδ for H3 and H5 and the bibliographic information mentioned above [34, 36], total inclusion may be concluded of PS in β-CD. On the other hand, given the size and conical shape of the β-CD cavity, different

Table 2. Proton ^{1}H-NMR chemical shifts corresponding to β-CD and inclusion complexes.

Nucleus	Chemical Shifts (δ) [ppm]		Δδ[b]
	β -CD (Free)	Inclusion Complexes[a]	
H-1	4.814	4.807	-0.007
H-2	3.300	3.315	0.015
H-3	**3.642**	**3.662**	**0.020**
H-4	3.331	3.324	-0.010
H-5	**3.561**	**3.582**	**0.021**
H-6	3.646	3.666	0.004
H-2´(OH)	5.660	5.648	-0.022
H-3´(OH)	5.660	5.645	-0.015
H-6´(OH)	4.440	4.375	-0.065

[a]Average values of the chemical shifts observed for inclusion complexes with different PS. $\Delta\delta^b = \delta_{(complex)} - \delta_{(\beta\text{-CD (free)})}$.

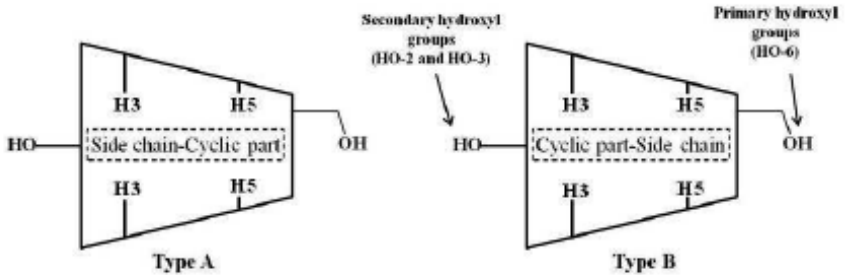

Fig. (7). Schematic representations of the conformations envisaged for the 1:1 (Types A and B).

types of the complex may have formed. As a first possibility, the side chain may be located toward primary alcohol groups outside the host (hydrophilic part); as a second possibility, the chain may be located close to the secondary face (hydrophobic part), inside β-CD. The remaining four types of complexes which could have been formed by one mole of host and guest [31] were ruled out considering the results obtained in mass spectrometry and elemental analysis. The results of the latter were used only to roughly estimate the composition of the sample.

Additionally, the values of Δδ for H3 and H5 of the free β-CD and the inclusion complexes may raise two structures in which each of the PS are included in the CD cavity.

Depending on guest conformations inside the host cavity, the cyclic part of PS may be closer to the small opening of the CD, with the side chain closer to the larger opening (Type A). A second option may be thought to have the opposite conformation (Type B) (Fig. **7**).

As the PS mixture used as starting material had βS as its main component and minor amounts of S and C, the reaction product did not prove to be a single inclusion, but a mixture of three complexes whose existence and identity were evidenced from the data obtained through ESI-HRMS. This tool proved highly useful due to structural similarity among the three guests, mainly in the case of βS and C, whose structural differences are based on the degree of substitution of the side alkyl chain linked to the cyclic part of PS. In contrast, the identification of S with reference to the other two PS was less complex, as the side chain presented unsaturation in position 22, whose identification yielded vital information from the two-dimensional NMR experiments.

As mentioned above, working on a PS mixture and their inclusion complexes rather than a single pure compound caused difficulty in NMR studies on samples. For these reasons, only partial proton and carbon attributions were obtained (Table **3**).

In order to perform a more detailed analysis, each PS, either free or being part of the inclusion complex, was divided in the form shown in Fig. (**1**), *i.e.* a cyclic part and a so-called side chain. Additionally, each spectrum was divided into six regions which can be observed in Fig. (**8**). The first spectral region between 0.6 and 0.7 ppm (Z1) contains the signals assigned to protons H18 (C), H18 (βS) and H18 (S). The second section (Z2) (0.7-0.85 ppm) contains the signals assigned to protons H28 (C), H26-27 and 29 of three PS. In a third zone (Z3) between 0.86 and 1 ppm approximately, signals can be assigned to protons H1a, H19 and H21, corresponding to three PS, as well as those signals assigned to protons H24 (βS and S) and H22a (βS and S). Between 3.20 and 3.30 ppm (Z4), signal was observed corresponding to proton H3 (βS, S, C). The signals assignable to the PS showing the greatest displacement (Z5) are those

Table 3. **^{1}H and ^{13}C NMR chemical shifts corresponding to free PS and inclusion complexes.**

Assignment[a] (^{1}H and ^{13}C)	^{1}H			^{13}C		
	Chemical Shifts (δ) [ppm]		Δδ	Chemical Shifts (δ) [ppm]		Δδ
	Free Phytosterols	Inclusion Complexes		Free Phytosterols	Inclusion Complexes	
1´a	0.968	0.966	-0.002	36.685	36.631	-0.054
2´a	1.323	1.320	-0.003	31.040	31.036	-0.004
2´b	1.670	1.655	-0.005			
3´	3.258	3.249	-0.009	69.773	69.714	-0.059
3´´(OH)	4.476	4.493	0.017	---	---	---
4´a-b	2.094	2.079	-0.015	41.916	41.858	-0.058
5´	---	---	---	140.925	140.970	0.045
6´	5.222	5.223	-0.001	12.240	120.428	0.008
7´a	1.888	1.888	0.000	31.091	31.001	-0.090
7´b	1.464	1.439	-0.025			
18C	0.629	0.631	0.002	11.301	11.512	0.201
18βS						
18S	0.649	0.651	0.002	11.450	11.693	0.243
19C	0.925	0.926	0.002	18.637	18.808	0.171
19βS						
19S	0.928	0.929	0.001			
20C	1.316	1.325	0.009	35.211	35.199	-0.012
20βS						
20S	1.995	2.006	0.011	39.680	39.683	0.003
21C	0.865	0.867	0.002	18.529	18.667	0.138
21βS	0.876	0.878	0.002	18.407	18.447	0.040
21S	0.973	0.975	0.002	20.698	20.688	-0.010
22S	5.114	5.117	0.003	137.843	137.875	0.032
22a βS-C	0.992	0.995	0.003	33.078	32.998	0.080
22b βS-C	1.282	1.290	0.008			
23S	4.980	4.978	-0.002	128.422	128.572	0.150
24βS	0.891	0.894	0.003	45.083	45.098	0.015
24S	1.488	1.488	0.000	50.364	50.323	-0.041
24C	1.163	1.164	0.001	37.997	38.006	0.009
25βS	1.616	1.612	-0.004	28.433	28.337	-0.096
25C	1.446	1.462	0.016	31.107	31.198	0.091
25S	1.325	1.379	0.044	31.091	31.244	0.153
26βS	0.792	0.795	0.003	19.444	19.429	-0.015
26C	0.725	0.731	0.006	17.063	17.132	0.069
27βS	0.771	0.774	0.003	18.520	18.554	0.034
28C	0.728	0.731	0.003	14.899	14.963	0.064
29βS	0.804	0.806	0.002	11.442	11.487	0.045
29S	0.758	0.751	-0.007	11.734	11.785	0.051
(26S, 27C-S)	0.735-0.820	0.740-0.840	0.005-0.020	----	----	----

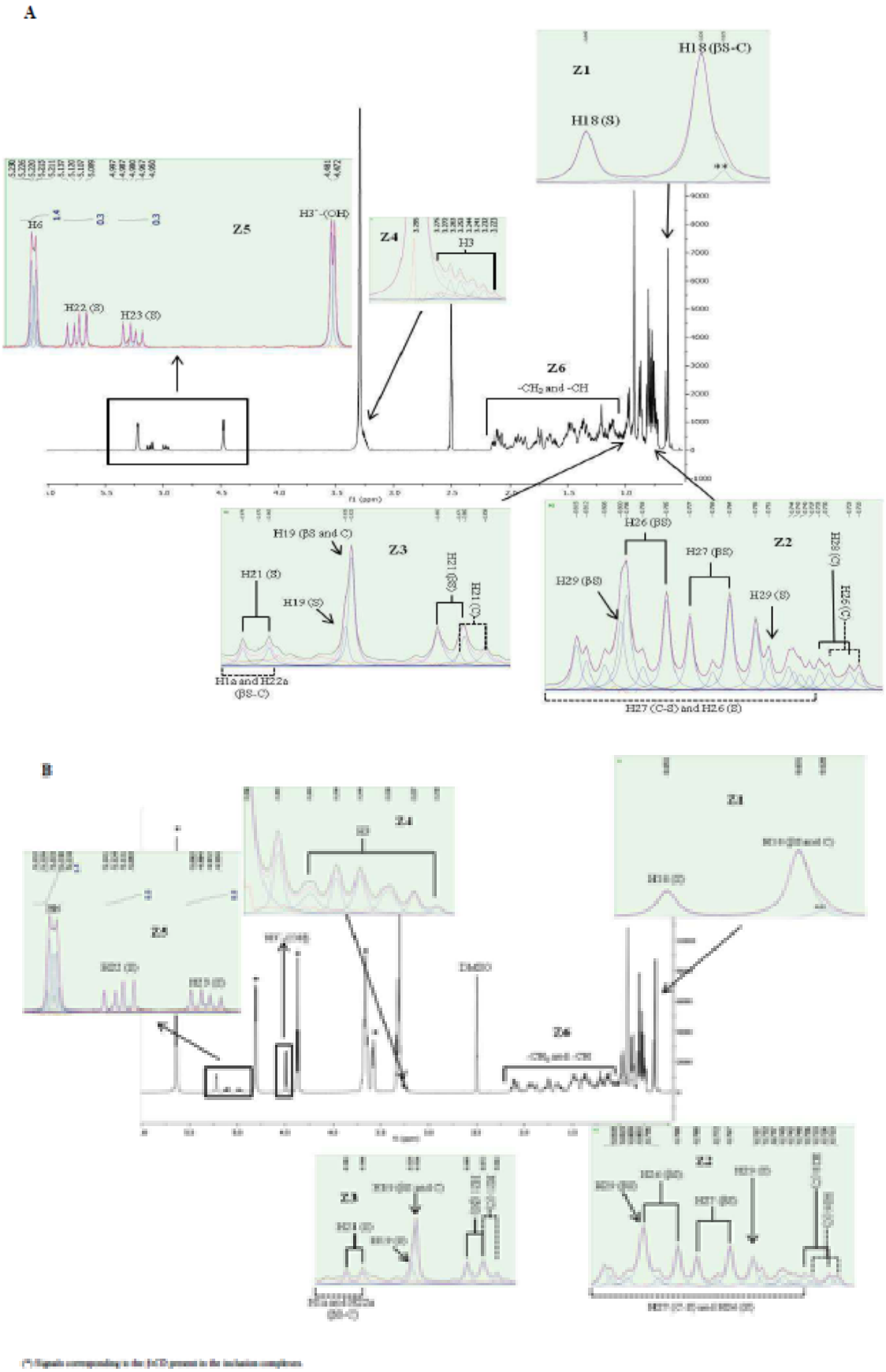

Fig. (8). A and B. ^{1}H-NMR spectra corresponding to free PS (top) and inclusion complexes (bottom).

corresponding to protons H22-23 (S), H3´(OH) and H6´, corresponding to three PS.

An automatic deconvolution analysis was performed on each of the zones, in order to improve the assignment accuracy and results in quality. Also, for validation purposes, a comparative analysis was carried out between the bibliographical information [32] on ^{1}H and ^{13}C NMR spectra performed on chloroform of the three PS separately and the PS mixture used here. It was possible to verify that the relative chemical displacements for the different nuclei of protons and carbons respected the same pattern of relative order in the zones mentioned above. The deconvolution analysis yielded similar results in the pattern of partition of signals and coupling constants, the only differences being observed in displacement values for the same nucleus, due to the effect of the solvent used. Therefore, given the consistency obtained, bibliographical data on magnetic resonance was used as an additional tool to the two-dimensional resonance spectra to perform the above-mentioned assignments.

Worth pointing out, the sixth zone analyzed (Z6) was that between 1.000 and 2.300 ppm, approximately, where the corresponding signals for the rest of proton nuclei which have not been previously mentioned can be found. Symbols (*) in Fig. (**8B**) indicate signals corresponding to the CD rather than PS.

The comparative analysis of region Z5 of ^{1}H-NMR spectra in Figs. (**8A** and **8B**) allowed to check for selectivity in the process of inclusion of S with respect to β-S. Results validity stemmed from the fact that the areas of the signals observed at 5.222 and 5.223 ppm in the spectra 8A and 8B, respectively, represent the total number of H6 proton nuclei present in cycle B of the three PS, while the areas of signals assigned to protons H22 (5.117 ppm) and H23 (4.978 ppm) correspond only to S. It should be made clear that comparison validity relies on a relative criterion, and that delay time used in the sequence of pulses to obtain spectra satisfied the condition that T_1 should be shorter than delay time between pulses.

The approximate proportions of inclusion complexes β-S and C derivatives and free PS mixture could not be assessed using a similar analysis as described above, as the signals corresponding to protons of β-S and C overlapped. In order to roughly calculate the relationship between H21 nuclei present in the Z3 region of the three PS in their free form (Fig. **8A**) and the corresponding inclusion complexes (Fig. **8B**), analyses focused on the areas of each signal obtained from the GSD, which revealed similar molar ratios of β-S, C and S before and after encapsulation.

In addition, the signals described above for regions Z1 and Z5 lead to the conclusion that the experimental conditions applied in the preparation of the inclusion complexes rendered a mixture with a percentage composition similar to that of free PS. These results confirm the absence of host selectivity about the PS components of the original mixture in the molar ratio used. As mentioned above, this lack of selectivity is considered an advantage, as a PS mixture could be encapsulated with a fixed component ratio which would not be affected by the inclusion reaction.

To continue with the analysis of the results obtained from the one- and two-dimensional NMR techniques, some concepts already described in the literature should be taken into account, namely:

a) Variations in the chemical displacements of the different nuclei, both in host and guest, are explained by the field theory, which interprets these findings as a consequence of the difference in dielectric environment [31,34b].

b) Complexes with aliphatic guest molecules lacking strong shielding tensors show only small and difficult to rationalize shielding effects on both host and guest. Nevertheless, the shift changes can be used not only to determine association constants but also [34b] to help determine possible intracavity inclusion.

c) The claim that $\Delta\delta$ H3 > $\Delta\delta$ H5 implies partial inclusion of the guest inside the cavity while $\Delta\delta$ H3 ≤ $\Delta\delta$ H5 implies total inclusion [32,34] may be based on the CD cavity shape. A higher degree of inclusion (defined, for the purposes of this work as the depth of insertion of the host molecule in the CD cavity of the host) means greater interaction with the H5 nucleus, which results in greater differences in the shift observed for this proton in the inclusion complex.

d) The interpretation of ^{13}C NMR screening changes poses obstacles associated to the pronounced sensitivity of carbon shielding toward even minor conformational distortions (Fig. **9**). Nevertheless, carbon atoms of guest molecules which are located deeper in the cavity generally seem to undergo shielding, whereas those closer to the large opening of the CD tend to be deshielded by complexation [31f,34b 38, 39].

e) Cholesterol was used as a model compound due to its similarities to PS (S, C and β-S), as far as the A-D cycles are concerned. On the basis of this analogy, bibliographical information can be found on the application of molecular modeling [40] in which cholesterol interacts with the β-CD in a conformation where cycle A is located in the small opening of the host cone, and a hydrogen bond can be formed between the H6´-(OH) and oxygen atom in the 3-position of the A cycle of the guest. This interaction should be reflected in a greater chemical shift for H3´´-(OH) nuclei, while H6´-(OH) nuclei may suffer an opposite effect. Provided the analogy used is valid, the same evidence should be obtained in the case of PS S, C and β-S.

Using the concepts mentioned in the analysis of the experimental data observed in one- and two-dimensional NMR spectra, Tables **2**, **3** and Fig. (**9**), we could extract important information referring to the form in which the different PS may interact with the β-CD. First, Table **2** shows that $\Delta\delta$ H3 (0.020 ppm) ≤ $\Delta\delta$ H5 (0.021 ppm), which, as mentioned above (concept c), allows to conclude that the degree of inclusion of the PS in the host was total, in agreement with models reported in the literature [32, 34]. The second interesting observation arises from the changes undergone by $\Delta\delta$

of H3´´-(OH) and H6´-(OH) (in absolute value). The magnitude of the changes might support the hypothesis of a Type A PS conformation (Fig. **7**). In addition, the sign of the displacements could coincide with the results obtained in the computational analysis reported for cholesterol, where a hydrogen bond might be generated between the oxygen atom located in the 3' position of the PS and the H6´-(OH) of β-CD [40]. Finally, the 13C NMR (Fig. **9**) and heteronuclear single-quantum correlation (HSQC) spectra of the complex mixture presented a single signal for each of the carbon nuclei.

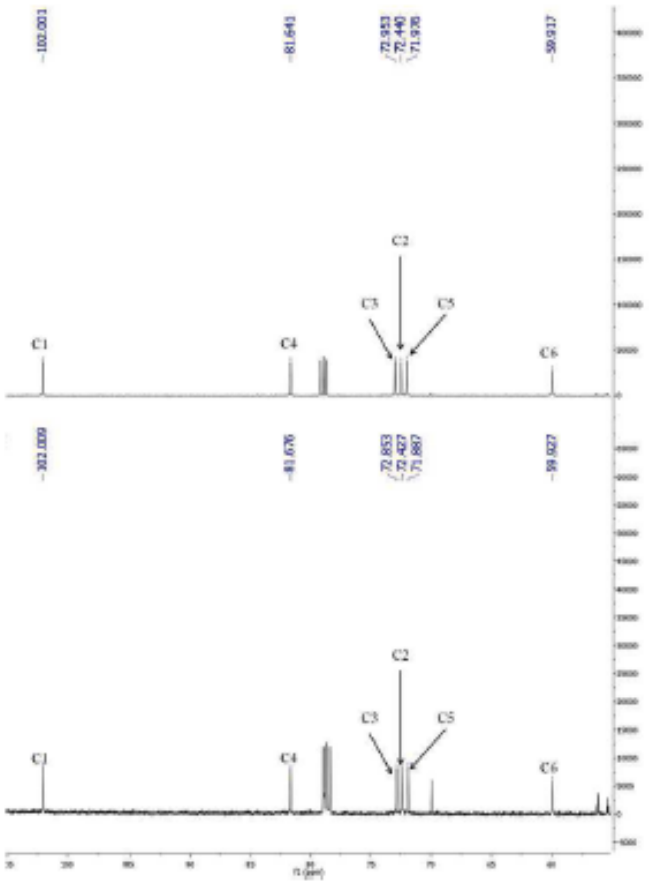

Fig. (9). ^{13}C NMR spectra corresponding to free β-CD (top) and inclusion complexes (bottom).

On the basis of these bibliographical data indicating that the variations in carbon chemical displacements present pronounced sensitivity of carbon shielding toward even minor conformational distortions [34b38, 39], it may be concluded that the conformations of each PS within the cavity of the β-CD were similar. Relating these experimental observations with respect to the host and concept d mentioned above, it could even be argued that the conformational changes generated by the inclusion of each PS were also similar. In addition, the greater variations in Δδ were those corresponding to the nuclei of carbon C-5 and C-3, which is consistent with the Δδ of H3 and H5. However, the latter is valid only when comparing variations corresponding to the C-bonded H nuclei, as the greatest variation was observed for nuclei H6´-(OH) (see Table **2** and Fig. **6A-B**).

To better understand this experimental evidence, an analogy could be considered in the interactions taking place between the H6´-(OH) nuclei of the β-CD and H3´´-(OH) of the PS. Indeed, the abnormal Δδ of the latter, considering the variance experienced by the rest of the hydrogen nuclei of the PS in their free form with respect to their encapsulated form (see Table **3**), may lead us to verify this hypothesis and accept β-CD/PS Type A interactions (Fig. **7**).

Accepting a Type A configuration of the β-CD/PS inclusion complexes critically requires the use of experimental and theoretical analytical tools to rationalize this finding as accurately as possible. A recent study [41] reports the formation of the β-CD/βS [inclusion complex using βS as starting material of technical grade and of the same brand as the one used in the present study, although no lot number is reported, which hinders the comparison of results. These authors only report the formation of the βS inclusion complex without reference to the behavior of other PS which may have been present in the starting material. Moreover, the work cited does not show the complete proton magnetic resonance spectra, which may have shown the presence or absence of signals corresponding to protons H23 and H22 corresponding to S, and the identification of other signals characteristic of S and C. However, the authors verify the stoichiometric ratio of β-CD/β-S in the inclusion complex by an experimental method different from that used in the present work. As a second relevant finding, the authors demonstrate by classical molecular dynamics calculations that the encapsulated cyclic head and complete encapsulated conformations were more stable than the encapsulated aliphatic tail.

In order to establish the type of complex formed between the β-CD and β-S, a comparative study was conducted between Ha-Hb correlations observed in nuclear Overhauser enhancement spectroscopy (NOESY) and rotating-frame nuclear Overhauser effect spectroscopy (ROESY) two-dimensional NMR spectra of free host and the inclusion complex. Basically, these two experiments were based on the fact that when two nuclei, Ha and Hb, are closely located, either in the same molecule or due to intermolecular forces, nuclei local fields will disturb one another causing a dipole-dipole coupling, which will have a null *J*-coupling but will change the spin-lattice relaxation time (T_1) in the inter-nuclei environment. This dipole-dipole coupling will cause the splitting of the spin energy levels of both Ha and Hb, which causes the so-called nuclear Overhauser effects (NOE), defined as the change in Ha resonance intensity when Hb resonance is altered [34a].

NOE measurements can be made in both steady and dynamic states. In the dynamic measurement, Hb resonance will not be saturated during the mixing time, and NOE enhancement will depend on both nuclei magnetization amplitudes after the evolution period t_1. The main difference with the NOESY experiment is that NOE intensity enhancement will be described as three different peaks in the two-dimensional spectrum, which can discriminate Ha-Hb cross-peak correlation from peaks related to other changes in Hb resonance [34a].

Another effect related to NOE, *i.e*. rotational Overhauser effect (ROE), gives rise to ROESY two-dimensional NMR spectra. The main advantage of ROESY experiments over

Table 4. Correlations H-H observed in NOESY and ROESY spectra of inclusion complexes.

Entry (E)	Correlation $Hn_{\beta\text{-}CD}/H_{Ph}$	NOESY	ROESY
1	$2/23_S$	+	
2	6/3´´-(OH)		+
3	$6/23_S$	+	
4	$1/18_{\beta S,S,C}$		+
5	$1/(26,27,21)_{\beta S,S,C}$	+	
6	3-(OH)/24C	+	
7	6´-(OH)/3´´-(OH)		+
8	$3/(26,27,21)_{\beta S,S,C}$		
9	$2´\text{-(OH)}/(26,27,21,19,18)_{\beta S,S,C}, 28_C, 29_{\beta S,S}$	+	+
10	$3´\text{-(OH)}/(26,27,21,19,18)_{\beta S,S,C}, 28_C, 29_{\beta S,S}$	+	+
11	$3/(26,27,21,19)_{\beta S,S,C}$		+
11*	$5/(26,27,21,19)_{\beta S,S,C}$		+
12	2/3´´-(OH)		+
13	5/ 3´´-(OH)	+	+
14	3/ 3´´-(OH)	+	
15	4/23		+
16	4/6´		+
17	3 and 5/1´a		+
18	5/3´	+	+
19	3/3´	+	+
20	3/2´a		+
21	5/2´a		+

traditional NOESY is the use of the spin-lock condition, which consists in applying a strong, constant and coherent pulse at Hb Larmor frequency throughout the mixing time.

This pulse will saturate the Hb resonance, as magnetization vector projections remain processing in the XY plane. Therefore, the ROE will not only be enhanced due to the longitudinal magnetization component interactions but also due to the interactions of transversal ones [34a], which makes ROESY suitable for structural studies of CD inclusion complexes.

Table **4** shows the signals corresponding to correlations ^{1}Ha-^{1}Hb observed in the NOESY and ROESY spectra (Fig. **10**). Assignments were made on the basis of COSY, HSQC and heteronuclear multiple-bond correlation (HMBC), and guest spectra data reported [32].

Table **4** shows only some proton-proton correlations out of the total observed in the NOESY and ROESY spectra. The most relevant correlations confirming our hypothesis of the existence of a Type A conformation were those corresponding to entries (E) 9-11*, 13-14 and 17-21. In turn, the multiple remaining correlations observed in both the NOESY and ROESY spectra (Fig. **10**) support the assumption that the lateral chain of the PS is folded in a certain way that allows its complete inclusion in the cavity of the CD, and thus give validity to the results obtained from the theoretical calculations reported.

3. EXPERIMENTAL

3.1. Materials

β-CD (CAVAMAX® W7) was from ISP Technologies, Inc. βS (practical grade) used as guest was from MP Biomedicals, Inc. (Lot. N° 6213K, Composition: β-S, ~40-60%; C ~20-40%; S~5%), containing β-S as the major product and minor amounts of S and C in terms of percentage by mass (% wt./wt.). All other reagents and solvents used were of analytical grade. All experiments were carried out using ultrapure water.

3.2. Inclusion Complex Preparation

β-CD (500 mg) was previously dissolved in 50 mL of distilled water at 40ºC in a water bath for the preparation of

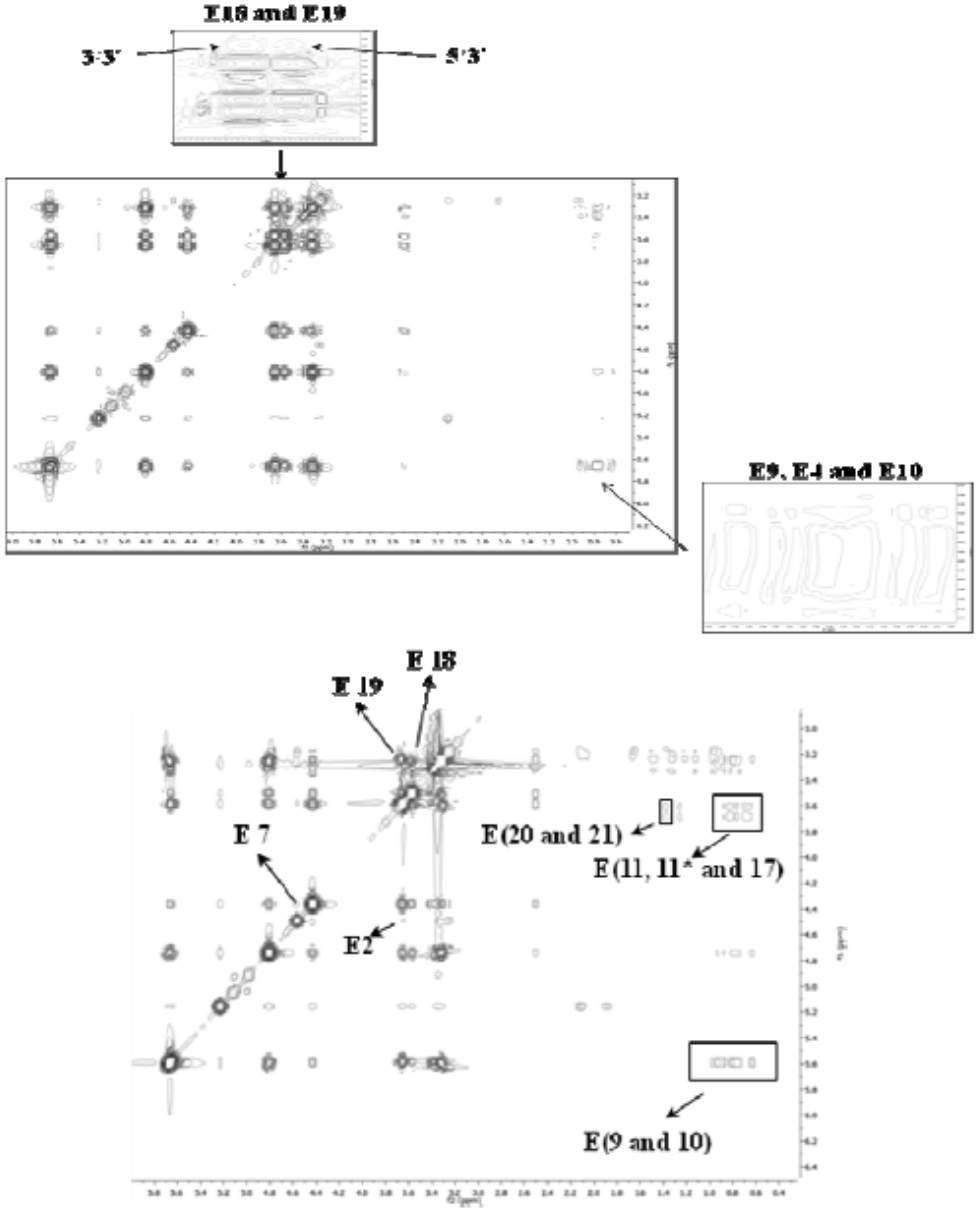

Fig. (10). NOESY (top) and ROESY (bottom) spectra of the inclusion complexes with H-H correlations of interest.

inclusion complexes. PS mixture (186 mg) was slowly added to β-CD water solution with continuous agitation (300 rpm). The vessel covered with aluminum foil was stirred continuously at the temperature indicated. The final solution was then refrigerated for 12 h at 5ºC. The precipitate complexes were recovered by filtration and dried, and the supernatant was lyophilized. Simultaneously, a physical mixture (PM) of β-CD and PS (molar ratio 1:1) was obtained as control by pulverization in a glass mortar. These powder samples were further analyzed by DSC, ESI-HRMS, IR spectroscopy and NMR.

3.3. GC Analysis

PS content was analyzed by GC on a Shimadzu GC 2012 Plus instrument, using a 30 m x 0.25 mm, i.d. 0.32 mm, 0.25-µm film thickness Equity-5 fused silica capillary column by Supelco. The flow rate of nitrogen as a carrier gas was 1.3 mL/min, split ratio was 1:10 (v/v) and temperature of injector and detector (FID) were 280 and 300°C, respectively. The oven temperature isotherm was 280°C. The sample injection volume was 1 µL.

3.4. β-CD Determination

Vikmon modified method was used to quantify β-CD [20]. This method is based on the decrease in absorbance at 550 nm due to the inclusion of phenolphthalein in β-CD. The decrease in absorbance is proportional to the amount of free β-CD. The working reagent was prepared with a stock solution of phenolphthalein 4 mM (1.0 mL), which was added ethanol (4.0 mL) and taken to 100 mL with a solution of 125 mM Na_2CO_3.

3.5. DSC Analysis

For DSC analysis of β-CD, PS, PM and the lyophilized samples, *i.e*. the inclusion complexes were measured on a Shimadzu DSC-50, scan rate 10/min, N2 atmosphere flow 50 mL/min, aluminum crimp crucible and final temperature 350°C. Analyses were performed at Instituto de Física La Plata, Universidad Nacional de La Plata (IFLP, UNLP), Argentina.

3.6 ESI-HRMS Analysis

High-resolution mass spectra resulting from ionization by electrospray in the positive mode were acquired on a Bruker micrOTOF-Q II mass spectrometer.

3.7. FT-IR Spectroscopy Analysis

FT-IR samples were prepared as KBr pellets, and their spectra determined on a Shimadzu IRPrestige spectrometer. Measurements were performed in the scanning range of 4000-400 cm^{-1}.

3.8. ^{1}H-NMR Analysis

One and two-dimensional NMR spectra were recorded on an Avance II Bruker 500 NMR spectrometer at 500 MHz. The β-CD, β-S/S/C mixture and supramolecular complexes were dissolved in DMSO-d_6/$CDCl_3$ (85:15). The measurement temperature was 298 K. Chemical shifts (δ) were reported in ppm and coupling constants (J) were reported in Hz. All one and two-dimensional spectra were recorded using the DMSO d_6 signals as a reference (2.500 and 39.520 ppm for ^{1}H and ^{13}C, respectively).

CONCLUSION

In this work, β-CD was applied as a successful carrier for the incorporation of PS. The formation of inclusion complexes between β-CD and the components of a PS mixture [34a] rich in β-S with minor amounts of S and C was confirmed and characterized by DSC, ESI-HRMS, FT-IR and one- and two-dimensional NMR techniques. The DSC thermogram of the solid inclusion complexes did not provide a sharp endothermic peak around the PS melting point, which was, however, present in the PM, demonstrating the molecular encapsulation of the PS inside the β-CD cavity. The 1:1 binding stoichiometry of the complexes was confirmed with ESI-HRMS examination. The data from ^{1}H-NMR and FT-IR analysis showed that it was feasible to obtain inclusion complexes of β-CD with the components of the PS mixture in the conditions established. Partial proof of the lack of selectivity in the inclusion process was obtained from the area ratio of signals corresponding to ^{1}H nuclei, which were analyzed by two-dimensional NMR. $\Delta\delta$ H3 (0.020 ppm) $\leq \Delta\delta$ H5 (0.021 ppm) showed the degree of inclusion of each PS in the host and suggested that rings and chains of β-S, S and C were included into the β-CD cavity. The multiple correlations observed in the NOESY and ROESY spectra support the assumption that the lateral chains of the different PS fold to reach total encapsulation.

CONSENT FOR PUBLICATION

Not applicable.

CONFLICT OF INTEREST

The authors declare no conflict of interest, financial or otherwise.

ACKNOWLEDGEMENTS

We acknowledge the financial support of Departamento de Ciencias Básicas and Secretaría de Ciencia y Tecnología, Universidad Nacional de Luján, Argentina. We would also like to thank P. Eng. Mariana Medanich and P. Eng. Mildred Cabrera from Laboratorio de Nutrición, Universidad Nacional de Luján, for their valuable assistance with the GC analyzed in the present study.

REFERENCES

[1] Srigley, C.T.; Haile, E.A. Quantification of plant sterols/stanols in foods and dietary supplements containing added phytosterols. *J. Food Comp. Anal.*, **2015**, *40*, pp 163-176.

[2] Laitinen, K.; Gylling, H. Dose-dependent LDL-cholesterol lowering effect by plant stanol ester consumption: clinical evidence. *Lipids Health Dis.*, **2012**, *11*, pp 140-146..

[3] Klingberg, S.; Ellegard, L.; Johansson, I.; Hallmans, G.; Weinehall, L.; Andersson, H. Inverse relation between dietary intake of naturally occurring plant sterols and serum cholesterol in northern Sweden. *Am. J. Clin. Nutr.*, **2008**, *87*, pp 993-1001 (Erratum: https://academic.oup.com /ajcn/article /96 /3/680 / 4576921).

[4] Plat, J.; Mensink, R.P. Plant Stanol and Sterol Esters in the Control of Blood Cholesterol Levels: Mechanism and Safety Aspects. *Am. J. Cardiol.*, **2005**, *96*, pp 15-22.

[5] Moreau, R.A.; Whitaker, B.D.; Hicks, K.B. Phytosterols, phytostanols, and their conjugates in foods: structural diversity, quantitative analysis, and health-promoting uses. *Prog. Lipid Res.*, **2002**, *41*, pp 457-500.

[6] Grattan, B.J. Jr. Plant Sterols as Anticancer Nutrients: Evidence for Their Role in Breast Cancer. *Nutrients*, **2013**, *5*, pp 359-387.

[7] Awad, A.B.; Chinnam, M.; Fink, C. S.; Bradford, P.G. β-Sitosterol activates Fas signaling in human breast cancer cells. *Phytomedicine*, **2007**, *14*, pp 747-754.

[8] Bin Sayeed, M. S.; Karim, S. M. R.; Sharmin, T.; Morshed, M. M. Critical Analysis on Characterization, Systemic Effect, and Therapeutic Potential of Beta-Sitosterol: A Plant-Derived Orphan Phytosterol. *Medicines*, 2016, *3*, pp 29-53, and references therein.

[9] Meng, X.H.; Pan, Q.Y.; Yang, T.K. Synthesis of Phytosteryl Esters by Using Alumina-Supported Zinc Oxide (ZnO/Al_2O_3) from Esterification Production of Phytosterol with Fatty Acid. *J. Am. Oil Chem. Soc.*, **2011**, *88*, pp 143-149.

[10] Leong, W.-F.; Lai, O.-M.; Long, K.; Che Man, Y.B.; Misran, M.; Tan, C.-P. Preparation and characterisation of water-soluble phytosterol nanodispersions. *Food Chem.*, **2011**, *129*, pp 77-83.

[11] Engel, R.; Schubert, H. Formulation of phytosterols in emulsions for increased dose response in functional foods. *Innov. Food Sci. Emerg. Technol.*, **2005**, *6*, pp 233-237.

[12] (a)Weber, N.; Weitkamp, P.; Mukherjee, K.D. Cholesterol-lowering food additives: lipase-catalysed preparation of phytosterol and phytostanol esters. *Food Res. Int.*, **2002**, *35*, pp 177-181. (b) Gonçalves, S.; Maria, A.V.; Silva, A.S.; Martins-Silva, J.; Saldanha C. Phytosterols in milk as a depressor of plasma cholesterol levels: experimental evidence with hypercholesterolemic Portuguese subjects. *Clin. Hemorheol. Microcirc.*, **2006**, *35*, pp 251-255. (c) Ruiu, G.; Pinach, S.; Veglia, F.; Gambino, R.; Marena, S.; Uberti, B.; Alemanno, N.; Burt, D.; Pagano, G.; Cassader, M. Phytosterol-enriched yogurt increases LDL affinity and reduces CD36 expression in polygenic hypercholesterolemia. *Lipids*, **2009**, *44*, pp 153-160. (c) Saraiva, D.; da Conceição Castilho, M.; do Rosário Martins, M.; da Silveira, M.I.N; Ramos, F. Evaluation of phytosterols in milk and yogurts used as functional foods in Portugal. *Food Anal. Methods*, **2011**, *4*, pp 28-34.

[13] Zhang, J.; Jiang, K.; An, K.; Ren, S.-H; Xie, X.; Jin, Y.; Lin, Y. Novel water-soluble fisetin/cyclodextrins inclusion complexes: Preparation, characterization, molecular docking and bioavailability. *Carbohydr. Res.* **2015**, *418*, pp 20-28.

[14] Silva, F.; Figueiras, A.; Gallardo, E.; Nerin, C.; Domingues, F. C. Strategies to improve the solubility and stability of stilbene antioxidants: A comparative study between cyclodextrins and bile acids. *Food Chem.* **2014**, *145*, pp 115-125.

[15] Pinho, E.; Grootveld, M.; Soares, G.; Henriques, M. Cyclodextrins as encapsulation agents for plant bioactive compounds. *Carbohydr. Polym.*, **2014**, *101*, pp 121-135.

[16] Ciobanu, A.; Landy, D.; Fourmentin S. Complexation efficiency of cyclodextrins for volatile flavor compounds. *Food Res. Int.*, **2013**, *53*, pp 110-114.

[17] Kurkov, S.; Loftsson, T. Cyclodextrins. *Int. J. Pharm.*, **2013**, *453*, pp 167-180.

[18] Astray, G.; Gonzalez-Barreiro, C.; Mejuto, J.C.; Rial-Otero, R.; Simal-Gándara, J. A review on the use of cyclodextrins in foods. *Food Hydrocoll.*, **2009**, *23*, pp 1631-1640.

[19] (a) Meng, X.; Pan, Q.; Liu, Y. Preparation and properties of phytosterols with hydroxypropyl β-cyclodextrin inclusion complexes. *Eur. Food Res.Technol*. **2012**, *235*, pp 1039-1047. (b) Uekama, K.; Fujinaga, T.; Hirayama, F.; Otagiri, M.; Yamasaki, M. Inclusion complexations of steroid hormones with cyclodextrins in water and in solid phase. *Int. J. Pharm.* 1982, *10*, 1-15. (c) Liu, F.-Y.; Kildsig, D.O.; Mitra, A.K. Beta-Cyclodextrin/Steroid Complexation: Effect of Steroid Structure on association equilibria. *Pharm. Res.* **1990**, *7*, pp 869-873.

[20] Wang, X.; Luo, Z.; Xiao, Z. Preparation, characterization, and thermal stability of β-cyclodextrin/soybean lecithin inclusion complex. *Carbohydr. Polym.*, **2014**, *101*, pp 1027-1032.

[21] Pralhad, T.; Rajendrakumar, K. Study of freeze-dried quercetin–cyclodextrin binary systems by DSC, FT-IR, X-ray diffraction and SEM analysis. *J. Pharm. Biomed. Anal.*, **2004**, *34*, pp 333-339.

[22] Guo, M.; Zhang, S.; Song,F.; Wang, D.; Liu, Z.; Liu; S. Studies on the non-covalent complexes between oleanolic acid and cyclodextrins using electrospray ionization tandem mass spectrometry. *J. Mass Spectrom.*, **2003**, *38*, pp 723–731.

[23] Guo, M.; Song, F.; Liu, Z..; Liu, S. Characterization of non-covalent complexes of rutin with cyclodextrins by electrospray ionization tandem mass spectrometry. *J. Mass Spectrom.*, **2004**, *39*, pp 594–599.

[24] Kwon, S.; Lee, W.; Shin; H.-J.; Yoon, S.-i..; Kim, Y.T.; Kim, Y.-J.; Lee, K.; Lee, S. Characterization of cyclodextrin complexes of camostat mesylate by ESI mass spectrometry and NMR spectroscopy. *J. Mol. Struct.*, **2009**, *938*, pp 192–197.

[25] Sagisaju, S.; Chen, K.; Cole, R.B.; Jursic, B, S. Electrospray-ionization mass spectrometry study of cyclodextrin complexes with A007 prodrugs. *Carbohydr. Res.*, **2009**, *344*, pp 2167–2172.

[26] Dipak, R.P.; Pravin, G.I.; Kripal, S.; Dipak, S.D. FTIR, ^{1}H NMR. Powder X-ray diffraction and DSC studies of "β-cyclodextrin-parachlorobenzonitrile" inclusion complex". *Res. J. Chem. Sci.*, **2012**, *2*, pp 60-63

[27] Li, N.; Liu, J.; Zhao, X.; Gao, Y.; Zheng, L.; Zhang, J.; Yu. Com plex formation of ionic liquid surfactant and β-cyclodextrin *Colloids Surf. A Physicochem. Eng. Asp.*, **2007**, *292*, pp 196–201.

[28] Li, W.; Lu, B.; Sheng, A.; Yang, F.; Wang, Z. Spectroscopic and theoretical study on inclusion complexation of beta-cyclodextrin with permethrin *J. Mol. Struct.*, **2010**, *981*, pp 194–203.

[29] (a) Szejtli, J. Introduction and General Overview of Cyclodextrin Chemistry. *Chem. Rev.*, **1998**, *98*, pp 1743–1754. (b) Ikuta, N.; Tanaka, A., Otsubo, A.; Ogawa, N.; Yamamoto, H.; Mizukami, T.; Arai, S.; Okuno, M.; Terao, K. ; Matsugo, S. Spectroscopic Studies of R(+)-α-Lipoic Acid—Cyclodextrin Complexes. *Int. J. Mol. Sci.,* **2014**, *15*, pp 20469-20485

[30] Crupi, V.; Majolino, D.; Venuti, V.; Guella, G.; Mancini, I.; Rossi, B.; Verrocchio, P.; Viliani, G.; Stancanelli, R. Temperature Effect on the Vibrational Dynamics of Cyclodextrin Inclusion Complexes: Investigation by FTIR-ATR Spectroscopy and Numerical Simulation. *J. Phys. Chem. A.*, **2010**, *114*, pp 6811–6817. (b) Ikuta, N.; Tanaka, A.; Otsubo, A.; Ogawa **.;** Yamamoto, H., i Mizukami, T; Arai A, Okuno, M.; Terao, K;. Matsugo S. Spectroscopic Studies of R(+)-α-Lipoic Acid—Cyclodextrin Complexes. *Int. J. Mol. Sci.* **2014**, *15*(11), pp 20469-20485.

[31] (a) Stothers, J.B. Carbon-13 NMR Spectroscopy, 1st Edition; Organic Chemistry, A Series of Monographs, Vol. 24. Academic Press: New York, **197**2. (b). Reichardt, C. Solvent Effects in Organic Chemistry. Verlag Chemie: New York, **1976**. (c) Ando, I.; Webb, G.A. Some quantum chemical aspects of solvent effects on NMR parameters. *Org. Magn. Reson.*, **1981**, *15*, pp 111-130. (d). Castagne, D.; Dive, G.; Evrard, B.; Frédérich, M.; Piel, G. Spectroscopic studies and molecular modeling for understanding the interactions between cholesterol and cyclodextrins. *J. Pharm. Pharmaceut. Sci.*, **2010**, *13*, pp 362-377. (e) Yanghong Li, B.S. Stereochemical Studies on the Metabolism of Sterols by Saccharomyces cervisiae Strain GL7. Mgr. Thesis [Online], the Graduate Faculty of Texas Tech University. Lubbock, TX., January1996.https://ttu-ir.tdl.org/ttu-ir/bitstream/handle/2346/17 003 / 31 295009804591.pdf?sequence=1 (accessed Feb 11, 2018). (f) Chaturvedula, V.S.P.; Prakash I. Isolation of Stigmasterol and β-Sitosterol from the dichloromethane extract of Rubus suavissimus. *Int. Curr. Pharm. J.*, **2012**, *1*, pp 239-242. (f) Sright, J.L.C.; Mclnnes, A.G.; Shimuzu, S.; Smith, D. G.; Walter, J. A..; Idler, D.; Khalil, W. Identification of C-24 alkyl epimers of marine sterols by ^{13}C nuclear magnetic resonance spectroscopy *Can. J. Chem*., **1978**, *56*, pp 1898-1903.

[32] Thakkar, A.L.; Demarco, P.V. Cycloheptaamylose inclusion complexes of barbiturates: Correlation between proton magnetic resonance and solubility studies. *J. Pharm. Sci.*, **1971**, *60*, 652–653.

[33] Greatbanks, D.; Pickford, R. Cyclodextrins as chiral complexing agents in water, and their application to optical purity measurements. *Magn. Reson. in Chem*., **1987**, *25*, 208-215.

[34] Pessine, F.B.T.; Calderini, .; Alexandrino, L. Review: Magnetic Resonance Spectroscopy, Kim, D., Ed.; INTECH, 2012; Chapter 12 Available from : http://www.intechopen.com/books/magnetic-resonance-spectroscopy/review-study-of-inclusion-complexes-with-cyclodextrins-by-mrs; and referen ces therein, (accessed, Feb 11,2018). (b) Schneider, H.-J.; Hacket, F; Rüdiger, V. NMR Studies of Cyclodextrins and Cyclodextrin Complexes. *Chem. Rev.* **1998**, *98*, pp 1755−1785.

[35] Xavier, C.R.; Silva, A.P.C.; Schwingel, L.C.; Borghetti, G.S.; Koester, L.S.; Mayorga, P.; Teixeira, H.F.; Bassani, V.L., Lula, I. S.; Sinisterra, R.D. Improvement of genistein content in solid genistein/-cyclodextrin complexes β. *Quim. Nova.* **2010**, *33*, pp 587-590.

[36] Cobas, C.; Seoane, F.; Domínguez, S.; Sykora, S.; Davies, A. N. A new approach to improving automated analysis of proton NMR spectra through Global Spectral Deconvolution (GSD). *Spectrosc. Eur.*, **2010**, *23*, pp 26–30.

[37] Airoldi, C; Tripodi, F.; Guzzi, C.; Nicastro, R.; Coccetti, P. NMR analysis of budding yeast metabolomics: a rapid method for sample preparation. *Mol. BioSyst.*, **2015**,*11*, pp 379-383.

[38] Inoue, Y. NMR Studies of the Structure and Properties of Cyclodex trins and Their Inclusion Complexes. *Annu. Rep. NMR Spectrosc.*, **1993**, *27*, pp 59-101.

[39] Gelb, R.I.; Schwartz, L.M.; Cardelino, B.; Fuhrman, H.S.; Johnson, R.F.; Laufer, D.A. Binding mechanisms in cyclohexaamylose complexes. *J. Am. Chem. Soc*., **1981**, *103*, pp 1750-1757.

[40] Jiang, H.; Zhang, S.; Shi, Q.; Jia, Y. 1H NMR investigation of supramolecular complex between β-cyclodextrin and cholesterol. *Wuhan Univ. J. Nat. Sci.*, **2011**, *16*, pp 79-82; and references therein.

[41] Cowins, J.; Abimbola, O.; Ananaba, G.; Wang, X.-Q.; Khan, I. Preparation and characterization of b-sitosterol/b-cyclodextrin crystalline inclusion complexes. *J. Incl. Phenom. Macrocycl. Chem.*, **2015**, *83*, pp 141-148.

[42] Goel, A.; Nene, S. N. Modifications in the Phenolphthalein Method for Spectrophotometric Estimation of Beta Cyclodextrin. *Starch/Starke*, **1995**, *47*, pp 399-400.